Title
Three-Electrode Study of Electrochemical Ionomer Degradation Relevant to Anion-Exchange-Membrane Water Electrolyzers

Journal
ACS Applied Materials & Interfaces, 14(16)

ISSN
1944-8244

Authors
Krivina, Raina A
Lindquist, Grace A
Yang, Min Chieh
et al.

Publication Date
2022-04-27

DOI
10.1021/acsami.1c22472

Peer reviewed

ACS APPLIED MATERIALS & INTERFACES

www.acsami.org

Research Article

Three-Electrode Study of Electrochemical Ionomer Degradation Relevant to Anion-Exchange-Membrane Water Electrolyzers

Raina A. Krivina, Grace A. Lindquist, Min Chieh Yang, Amanda K. Cook, Christopher H. Hendon, Andrew R. Motz, Christopher Capuano, Katherine E. Ayers, James E. Hutchison, and Shannon W. Boettcher*

Cite This: *ACS Appl. Mater. Interfaces* 2022, 14, 18261−18274

Read Online

ACCESS | Metrics & More | Article Recommendations | Supporting Information

ABSTRACT: Among existing water electrolysis (WE) technologies, anion-exchange-membrane water electrolyzers (AEMWEs) show promise for low-cost operation enabled by the basic solid-polymer electrolyte used to conduct hydroxide ions. The basic environment within the electrolyzer, in principle, allows the use of non-platinum-group metal catalysts and less-expensive cell components compared to acidic-membrane systems. Nevertheless, AEMWEs are still underdeveloped, and the degradation and failure modes are not well understood. To improve performance and durability, supporting electrolytes such as KOH and K_2CO_3 are often added to the water feed. The effect of the anion interactions with the ionomer membrane (particularly other than OH^-), however, remains poorly understood. We studied three commercial anion-exchange ionomers (Aemion, Sustainion, and PiperION) during oxygen evolution (OER) at oxidizing potentials in several supporting electrolytes and characterized their chemical stability with surface-sensitive techniques. We analyzed factors including the ionomer conductivity, redox potential, and pH tolerance to determine what governs ionomer stability during OER. Specifically, we discovered that the oxidation of Aemion at the electrode surface is favored in the presence of CO_3^{2-}/HCO_3^- anions perhaps due to the poor conductivity of that ionomer in the carbonate/bicarbonate form. Sustainion tends to lose its charge-carrying groups as a result of electrochemical degradation favored in basic electrolytes. PiperION seems to be similarly negatively affected by a pH drop and low carbonate/bicarbonate conductivity under the applied oxidizing potential. The insight into the interactions of the supporting electrolyte anions with the ionomer/membrane helps shed light on some of the degradation pathways possible inside of the AEMWE and enables the informed design of materials for water electrolysis.

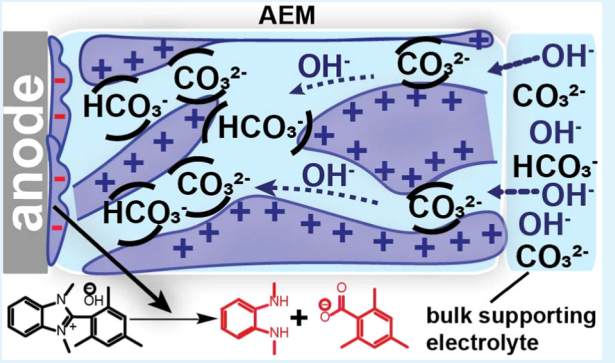

KEYWORDS: *anion-exchange-membrane water electrolysis, ionomer, supporting electrolyte, XPS, electrochemical degradation*

1. INTRODUCTION

Water electrolysis has the potential to provide clean H_2 from renewable electricity for heating, powering transport, chemical production, and metal refining.[1] To compete with fossil fuels, H_2 must be low cost (probably <$2/kg) and produced at scale.[2,3] Improving efficiency and durability while dramatically lowering the capital cost of electrolyzers is key to implementing sustainable H_2 production on a scale commensurate with energy needs.

Anion-exchange-membrane water electrolyzers (AEMWEs) are a newer technology that has potential to overcome the weaknesses of more mature electrolyzer technologies, such as proton-exchange-membrane water electrolyzers (PEMWEs) and alkaline water electrolyzers (AWEs).[4,5] AEMWEs adapt the compressed stack design of PEMWEs to produce pressurized H_2 but use a solid OH^--conducting anion-exchange polymer membrane that creates a locally basic environment for the cathode and anode catalysts.[2,6] A sheet of the solid AEM (typically 20−80 μm in thickness) is placed between the anode and cathode electrodes, while a soluble or dispersed form of the AEM polymer, the ionomer, is mixed in the catalyst ink to improve ionic and physical contact between the membrane and the catalyst-covered electrodes. Such membranes/ionomers, in principle, allow the use of non-platinum-group (non-PGM) catalysts that are superior to IrO_2 in alkaline pH for water oxidation and avoid using concentrated KOH, ideally pumping pure water through the system instead for the lower balance of plant costs.[7−9]

Received: November 19, 2021
Accepted: March 29, 2022
Published: April 18, 2022

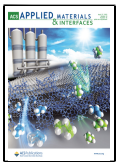

AEMWEs are still under development, and their durability is inferior to PEMWEs and AWEs.[2] The existing AEMs are generally not as physically and chemically robust as Nafion used in PEMWEs, and they suffer from insufficient ionic conductivity during operation.[2,10] To mitigate ohmic losses, particularly in the catalyst/ionomer reaction layer, supporting electrolytes such as 0.1−1.0 M KOH or K_2CO_3 have been added to the AEMWE feed. Addition of an electrolyte improves performance but introduces other issues.[6,11−13] Performance loss pathways remain difficult to identify, and, thus, an informed design of the cell components is challenging.

The interface between the catalyst and ionomer binder comprises the reactive zone at the anode and is likely the weakest point in the system due to the highly oxidizing potential.[14,15] Being in direct contact with the anode catalyst surface, the ionomer would be the first to sustain any chemical changes due to oxidation.[16] The oxidation of the ionomers under applied potential has been shown to lead to the formation of new chemical structures, a change in local pH at the catalyst surface, and consequent catalyst loss.[16−19]

In the presence of a supporting electrolyte containing carbonate, the degradation modes may be more complicated. The presence of carbonate anions instead of OH^- might lead to a steeper pH gradient within the membrane. The understanding of the anion interactions and their effect on the stability of the ionomer/membrane during operation in a supporting electrolyte containing anions other than OH^- is limited.[12,16,20]

Here, our results suggest that the identity of the anions that transport through the ionomer binder during electrolysis and their interactions with the charged groups within the polymer can facilitate ionomer degradation. We illustrate possible degradation modes of ionomers in supporting electrolytes to understand the interactions of anions with the ionomers possessing different chemical structures. We focus on three high-performance commercial ionomers, Aemion by Ionomr,[21] Sustainion by Dioxide Materials,[22] and PiperION by Versogen[23] (Figure 1), with common supporting electrolytes under oxidizing applied potentials. Because different catalyst surfaces have been observed to promote ionomer degradation,[16] we do not add catalyst to the ionomers but instead test them on planar metal electrodes across all experimental degradation measurements. We analyze the effects of the anions' identity on their transport through the ionomers and track the changes to the chemical structures of the ionomers as the potential increases. We use density functional theory (DFT) calculations to estimate trends in redox potentials and visualize predicted highest occupied molecular orbitals (HOMOs) located on the conjugated components of each ionomer. This work thus provides insight into the nature of the interactions of the various anions with the ionomers/membranes, helps us to assess its effects, and illustrates the structure−stability relationship for the different supporting electrolytes. Particularly, this work is relevant for designing more chemically stable ionomers and identifying the best ionomer for an AEMWE given the supporting electrolyte used.

2. EXPERIMENTAL SECTION

2.1. Materials. Sustainion-XA9 and PiperION (PAP-TP-85) ionomer solutions in ethanol (5 wt %) were used as received from Dioxide Materials and Versogen, respectively. Aemion (AP1-HNN8-00-X) by Ionomr dry powder was received and dissolved in ethanol to obtain a 5 wt % solution. Supporting electrolytes were prepared using

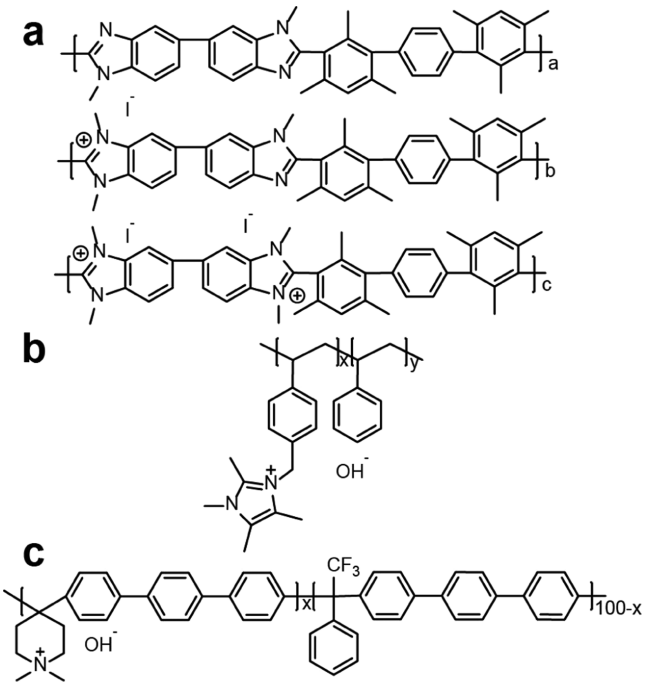

Figure 1. Chemical structures of (a) Aemion by Ionomr, (b) Sustainion by Dioxide Materials, and (c) PiperION by Versogen.

KOH pellets (Fischer Chemical, ≥85.0%), K_2CO_3 (Fischer Chemical, ≥99.0%), $KHCO_3$ (Fischer Chemical, ≥99.7%), NaOH (Fischer Chemical, ≥97.0%), H_3BO_3 (Mallinckrodt, ≥99.5%), and perchloric acid (60−62%, J. T. Baker Chemical, ACS grade) dissolved in 18.2 MΩ·cm H_2O.

2.2. Electrochemical Measurements with a Quartz Crystal Microbalance (QCM). Ionomer solutions at 5 wt % were spin-coated at 3000 rpm onto 5 MHz Au/Ti quartz crystals (QCs, Fil-Tech) and annealed at 80 °C for 15 min. Aemion films were then soaked in 1 M NaCl for 1 h to ion-exchange the I^- counterion for Cl^-. Sustainion films were soaked in 1 M KOH for 1 h after annealing. PiperION films were soaked in 1 M HCl for 5 min immediately after spin-coating and then rinsed with 18.2 MΩ·cm H_2O and annealed at 80 °C. Prior to electrochemical testing, the PiperION films were also soaked in 0.5 M NaOH for 15 min (see the discussion on the preconditioning of the selected ionomers in the Supporting Information). A BioLogic SP300 potentiostat was used operating in a three-electrode mode. A Pt coil was used as the counter electrode, while the Au/Ti QC with ionomer films on top served as the working electrode connected to the QCM controller (Stanford Research Systems QCM200) for monitoring mass changes during electrochemical testing. Potentials in three-electrode modes were measured vs a 1 M KOH Hg/HgO reference electrode (CH Instruments). The cell was degassed with N_2 prior to electrochemical testing. High-purity N_2 was bubbled in the electrolyte during the experiment.

The ionomer films were tested in three electrolytes: 1 M KOH (pH 14), 1 M carbonate/bicarbonate buffer (pH 10), and 1 M borate buffer (pH 8). In each supporting electrolyte, the films were first held at the open circuit voltage (OCV) for 2 h, and then a series of overpotentials (relative to the reversible oxygen potential in that electrolyte) were applied (η = 400, 500, 600, and 700 mV) for 1 h each. The films were then held at the OCV again for 1 h. The changes to the QCM resonance frequency during the chronoamperometry were converted to percent mass loss relative to the initial masses of the fresh films in each supporting electrolyte. The films' thicknesses were calculated using the ionomers' densities provided by the manufacturers, the known area of the Au/Ti electrode, and the film's mass calculated from changes in resonance frequency using the Sauerbrey equation:[24] $\Delta f = -C_f \times \Delta m$, where Δf is the observed frequency change (Hz), C_f is the sensitivity factor of the 5 MHz AT-

https://doi.org/10.1021/acsami.1c22472
ACS Appl. Mater. Interfaces 2022, 14, 18261−18274

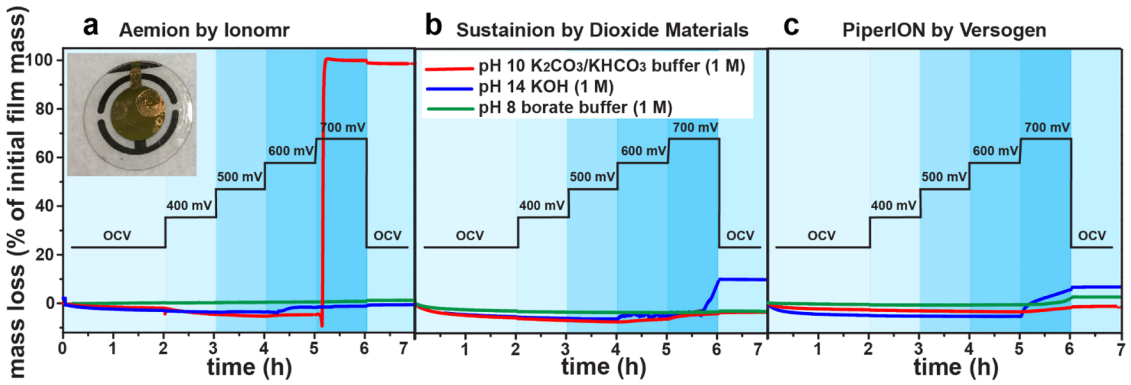

Figure 2. Dissolution of ionomer films under applied potential. The mass changes were monitored for 7 h in 1 M KOH (blue traces), 1 M carbonate/bicarbonate buffer (red traces), and 1 M borate buffer (green traces) for (a) Aemion by Ionomr, (b) Sustainion by Dioxide Materials, and (c) PiperION by Versogen. The data is plotted as the percentage of mass loss relative to the initial mass of an ionomer film immersed in the electrolyte. The overpotentials are referenced to E_{OER} at the pH of the electrolytes. The open circuit voltage (E_{ocv}) ranges measured for each electrolyte are E_{ocv} = −0.5 to −0.6 V vs E_{OER} at pH 10, E_{ocv} = −0.4 to −0.2 V vs E_{OER} at pH 14, and E_{ocv} = −0.6 to −0.1 V vs E_{OER} at pH 8 (these values are ranges because the electrolyte is devoid of redox species capable of setting the electrode potential). Inset: Aemion film flaking off a quartz crystal after electrochemical testing in carbonate consistent with oxidative damage at the electrode/ionomer interface.

cut quartz crystals (56.6 ± 3.7 Hz·μg^{-1}·cm^2), and Δm is the change in mass per unit area (μg·cm^{-2}). A Dektak 6M stylus profilometer was used to confirm the calculated film thickness (see Table S1 for the summary of the thicknesses).

2.3. Thin Film Characterization by X-ray Photoelectron Spectroscopy (XPS). Pt/Ti-coated glass slides (1 cm × 1 cm) were cleaned by O_2 plasma and rinsed with ethanol at 3000 rpm. The 5 wt % ionomer solutions were diluted to 0.16 wt % with ethanol and spin-coated on the Pt/Ti-coated glass substrates at 3000 rpm and annealed at 80 °C for 15 min. Aemion films were soaked in 1 M NaCl for 1 h after drying on the hot plate. Sustainion films were soaked in 1 M KOH for 1 h after annealing. PiperION films were soaked in 1 M HCl for 3 min immediately after spin-coating and then rinsed with 18.2 MΩ·cm H_2O and dried. The ionomer-covered substrates were fabricated into electrodes by making an ohmic contact with the Pt surface with a Cu-wire coil and Ag paint. The coil was then fixed in a 5-inch glass tube. The contact and the tube were insulated by epoxy (Loctite 9460) and cured in the oven. The electrodes were tested in a similar three-electrode cell as the Au/Ti quartz crystal electrode, but a new electrode was used for each overpotential. The cell was degassed with N_2 prior to electrochemical testing. High-purity N_2 was bubbled in the electrolyte during the experiment. The films were held at the OCV for 20 min before the potential was applied for 1 h in each of the three supporting electrolytes. The working electrode was then taken out, and the film was rinsed with copious amounts of water and dried at 80 °C for 1 h. PiperION substrates were soaked in 1 M HCl for 3 min after electrochemical testing before they were dried. Each film was analyzed with X-ray photoelectron spectroscopy (XPS) on an ESCALAB 250 (Thermo Scientific) using an Al Kα monochromated (20 eV pass energy, 500 μm spot size) source. The samples were charge-neutralized using an in-lens electron source. Spectra were analyzed using Thermo Scientific Avantage 4.88 software. The C 1s signal at 284.8 eV was used to calibrate the binding energy scale (see Table S2 for the summary of peak fitting). A similar test was carried out with the three ionomer films using 0.1 M $HClO_4$ as electrolyte at η = 400 and 600 mV. The films tested in acid were also analyzed with XPS.

2.4. Attenuated Total Reflectance Measurements on Postmortem Ionomer Films. Au/Ti-coated glass slides (3 cm × 3 cm) were cleaned by O_2 plasma and rinsed with ethanol at 3000 rpm. The 5 wt % ionomer solutions were spin-coated on the Au/Ti-coated glass substrates at 3000 rpm and annealed at 80 °C for 15 min. Aemion films were soaked in 1 M NaCl for 1 h after annealing. Sustainion films were soaked in 1 M KOH for 1 h after annealing. PiperION films were soaked in 1 M HCl for 5 min immediately after spin-coating and then rinsed with 18.2 MΩ·cm H_2O and annealed. Prior to electrochemical testing, the PiperION films were also soaked in 0.5 M NaOH for 15 min. The ionomer-covered substrates were fabricated into electrodes as described previously. The electrodes were tested in a similar three-electrode cell as above, but after applying each overpotential for 1 h, the electrode was taken out, rinsed with copious amounts of water, dried at 80 °C for 30 min (the PiperION film was soaked in 1 M HCl for 5 min prior to drying to remove OH^- that would damage the film in the dry state), and analyzed by collecting an attenuated total reflectance (ATR) spectrum (200 scans) using Smart *i*TR accessory equipped with a diamond crystal on a Thermo Fischer Nicolet 6700 spectrometer (4000−400 cm^{-1}) with a resolution of 6 cm^{-1}. The same substrate was then fabricated into an electrode again to be tested at the next highest overpotential in the same supporting electrolyte.

2.5. Computations. Density functional theory (DFT) was used to assess both the oxidation potentials and vibration properties of representative portions of Sustainion, PiperION, and Aemion. To do so, a hybrid-GGA method was used, PBE1PBE/6-31+G*. The redox potential was computed using a previously reported method,[25] with a computational standard hydrogen electrode value of −4.44 eV. The truncated portions of the polymers were created by passivating cleaved sp^3-carbon bonds with charge compensatory protons. Both *cis* and *trans* conformations of Sustainion were examined. For the larger polymers, PiperION and Aemion, the polymer was truncated to exclude cationic portions of the polymer (i.e., the portion with very large oxidation potentials). A pseudo-solvent was included in the computations using the self-consistent reaction field approach, with the polarizable continuum model (solvent = water), simulated at 293 K. Frequencies were used to confirm that truncated geometries are at least metastable, and the computed vibrations were scaled by 0.981 to account for the DFT approach used herein.

3. RESULTS AND DISCUSSION

The ionic radius and hydration energy of ions have been shown to govern ion transport through anion-exchange membranes.[26] The anions with lower hydration energy adsorb onto the membrane more easily but diffuse slower.[26] Adsorption refers to the process of anion partial dehydration and formation of an electrostatic bond to the charged groups on the membrane surface. The overall size of the anion and its geometry also influence the adsorption of anions and the rate of diffusion through the membrane. Given these findings, anions strongly interacting with the cationic ionomer groups might accumulate in the membrane, lowering OH^- concentration and thus conductivity, which can negatively affect the ionomer/membrane stability.

https://doi.org/10.1021/acsami.1c22472
ACS Appl. Mater. Interfaces 2022, 14, 18261−18274

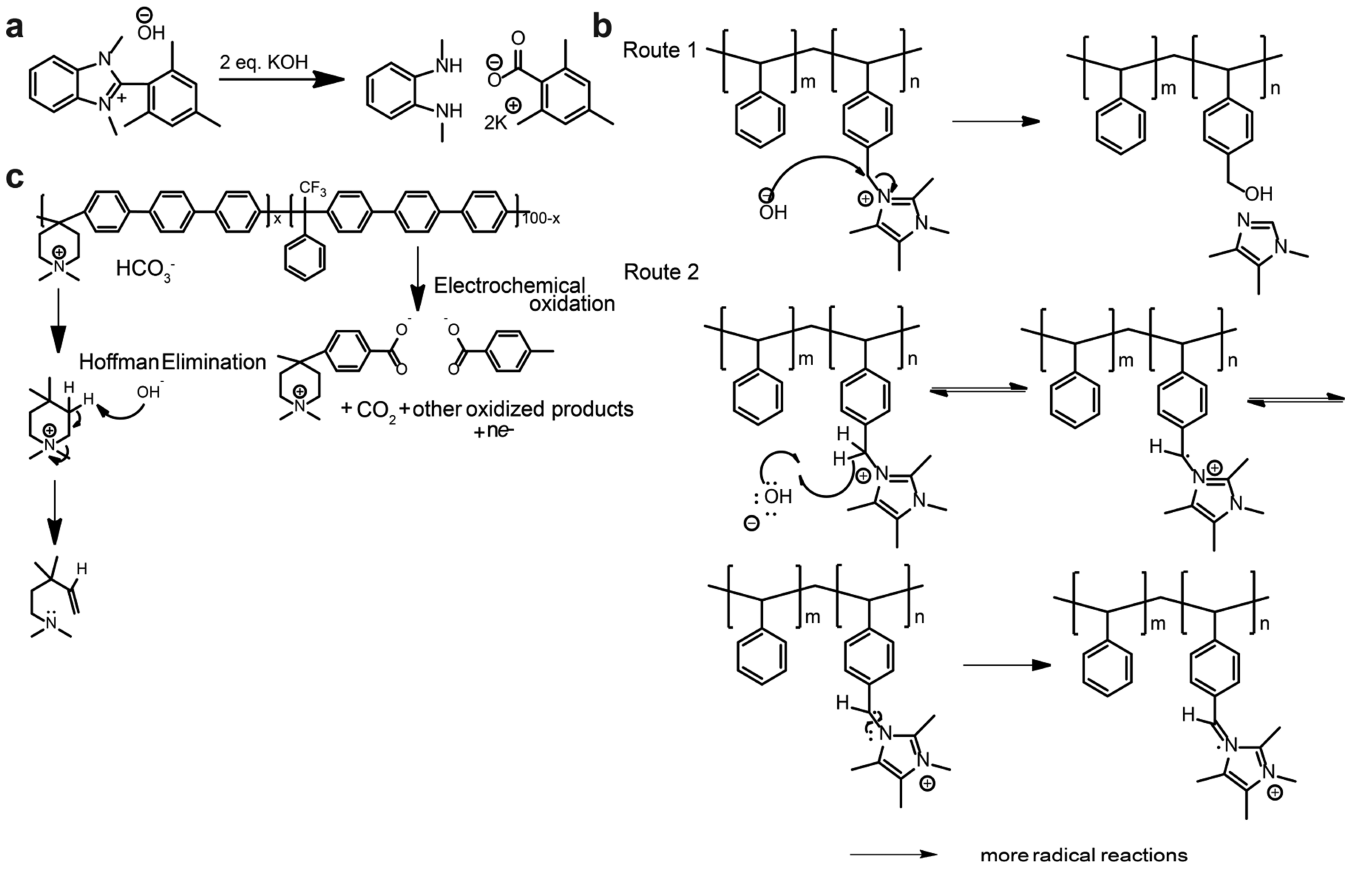

Figure 3. Chemical and electrochemical degradation routes for the studied ionomers. (a) Aemion is hypothesized to undergo degradation through nucleophilic displacement or a nucleophilic OH^- attack on the benzimidazolium C_2-position that leads to the ring opening. (b) Sustainion can also be subject to the imidazolium ring opening or undergo an OH^- attack at the α-carbon joining the imidazole and the phenyl group. (c) PiperION likely suffers from Hoffman β-elimination and S_N2-methyl substitution in the piperidinium ring. Electrochemical degradation (shown only for PiperION) is possible for all three polymers through the attack of reactive oxygen species ($HO^{\cdot}$, $HO_2^{\cdot}$, O_2^{-}) that are produced as OER intermediates or as a consequence of other electrochemical reactions under applied oxidative potential.

To gain insight specifically into the ionomer/supporting anion interactions under anodic applied potentials, we studied simplified thin film model systems of commercial ionomers (Aemion by Ionomr, Sustainion by Dioxide Materials, and PiperION by Versogen) on Au/Ti and Pt/Ti electrodes in three supporting electrolytes (pH ~14, 1 M KOH; pH ~10, 1 M K_2CO_3/$KHCO_3$ buffer; and pH ~8, 1 M borate buffer) under a range of applied potentials. The specific versions of the ionomer were chosen because they appear frequently in the literature and their structure and properties are well known. We recognize that newer materials might be available from Ionomr, Dioxide Materials, and Versogen (for instance, Aemion$^+$)[18,27] that we did not include in our study due to their unavailability during the initial stages of the work. No catalyst powder was added to avoid catalyst-surface-specific degradation. Borate buffer (pH 8) was selected as the third supporting electrolyte because, at this pH and concentration, the aqueous species in the buffer exist mostly as a triborate cluster ($3B(OH)_3 \leftrightarrow B_3O_3(OH)_4^- + H^+ + 2H_2O$).[28] While this electrolyte provides a less basic pH, the bulky triborate clusters are unlikely to adsorb and diffuse through the ionomer films and affect the internal pH.[29] The anions' ionic radii, geometries, and hydration energies are summarized in Table S2.

3.1. Tracking Ionomers' Dissolution under Applied Potential. To assess the ionomers' stability in the selected electrolytes under increasing oxidizing potentials, thin ionomer films (see Table S1 for thicknesses) were spin-coated from the 5 wt % ionomer solutions on Au/Ti quartz crystal electrodes. Figure 2 shows the changes in the films' mass under increasing overpotential (overpotential η is the excess potential beyond the thermodynamic potential required for the water oxidation reaction to occur, reported in mV vs E_{OER} at a given pH).

Initially at the open circuit voltage when no current flows (OCV), the films were observed to gain mass (Figure 2). This is likely due to the hydration of the films as well as counterion exchange that further leads to water entering the polymer. In borate buffer, this mass increase was the smallest for all ionomer films. This result supports the initial hypothesis that the triborate clusters[28] have difficulty diffusing through the film compared to OH^- and CO_3^{2-}/HCO_3^-.

Films tested in the borate buffer also did not yield any mass losses under applied oxidizing potentials, even at the highest overpotential. In the KOH electrolyte, the ionomer films took up water and increased in mass at the OCV. At η = 700 mV, Sustainion and PiperION lost ~5−10% of their mass. Aemion appeared to lose some of the mass gained during hydration and initial ion exchange at η = 600 mV. These mass changes might be indicative of the ionomer dehydration or the initiation of a degradation process. In K_2CO_3/$KHCO_3$ buffer, the difference between the mass losses observed for Aemion, Sustainion, and PiperION was significant. Neither Sustainion nor PiperION

https://doi.org/10.1021/acsami.1c22472
ACS Appl. Mater. Interfaces 2022, 14, 18261−18274

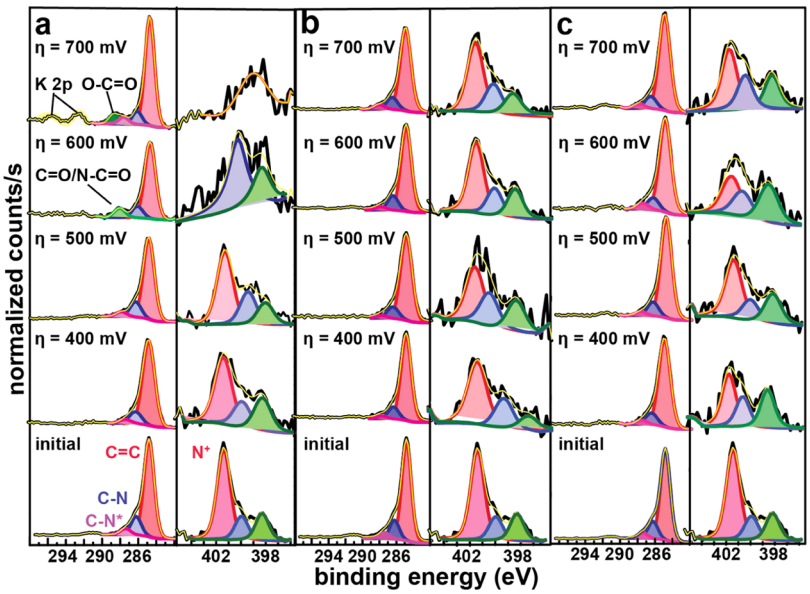

Figure 4. Structural changes to the Aemion film in three supporting electrolytes. XP spectra of C 1s and N 1s of Aemion thin films as Aemion changes under increasing applied potential in (a) pH 10, 1 M K_2CO_3/$KHCO_3$ buffer; (b) 1 M KOH; and (c) pH 8, 1 M borate buffer. Because the thin polymer films might sustain beam damage during prolonged XPS analysis, we tested if the C 1s spectra of the ionomers changed as we increase the number of scans on the same spot (Figure S1). We did not observe any changes caused by the increase in the number of scans for the three ionomer films. Thus, peaks observed by XPS in the thin film samples tested under applied potentials are unlikely to be the result of beam damage.

lost mass. The Aemion film was completely lost at η = 700 mV after just a few minutes (Figure S2 for the Aemion film that was preconditioned differently in an attempt to improve stability). Ionomer films are known to deadhere from a surface during ion exchange,[30] but this is unlikely the cause given the time at OCV allowing for ion exchange into the HCO_3^-/CO_3^{2-} form. It is possible that the origin of the film loss is a chemical change to the structure of the ionomer that caused the portion of the film directly in contact with the electrode to become soluble. The inset in Figure 2 shows an Aemion film starting to flake off at η = 600 mV. Based on this observation, we conclude that the interface of the ionomer film directly in contact with the electrode surface oxidizes, increasing solubility and decreasing adhesion to the surface, while the rest of the film is intact. The solubility of the fragment directly in contact with the electrode causes the films to flake off.

The information that can be obtained from the QCM is limited to the mass changes. Thus, to investigate chemical degradation occurring in the system, additional characterization techniques were employed. Due to the thinness of the ionomer layers, common techniques used to access the stability of thick solid membranes, e.g., tensile strength or ion-exchange capacity measurements, were not possible. Therefore, we analyzed the ultrathin polymer films with surface-sensitive characterization techniques to assess this interfacial region where degradation was hypothesized.

3.2. Tracking Structural Changes in Thin Ionomer Films with XPS. XPS was used to track changes to the structures of the three studied ionomers in the different supporting electrolytes. To obtain thinner ionomer films, the ionomer solution was diluted to 0.16 wt %. The resulting film thicknesses were 18, 9, and 12 (±1 nm) for Aemion, Sustainion, and PiperION, respectively. Using such thin polymer films allows us to gain the information about structural changes occurring at the interface of the electrode surface with ionomer and would not be possible on thicker membranes. However, this approach eliminates the ability to easily measure the films' ion-exchange capacity and conductivity, which are common and useful descriptors of the membrane stability. These descriptors require measurements of mass and volume along with typically measuring the ionomer in a two-probe station, which is difficult with very thin films due to lack of mechanical strength.

We also tested our hypothesis that the triborate clusters ($B_3O_3(OH)_4^-$) present in the pH 8 borate buffer would not interact within the ionomer films. Boron has a low XPS sensitivity factor (0.49; for comparison, the sensitivity factor of C is 1.0 and N is 1.8).[31] To determine if any boron-containing species diffused in the films, we used thicker ionomer films spin-coated from a 5 wt % solution and tested them at η = 600 mV in borate buffer. The B 1s peak was collected with a 75 eV pass energy, and the B/C ratio in the film was calculated. For Aemion, Sustainion, and PiperION, the B/C ratios were 0.3, 0.3, and 0.1%, respectively. That same nominal amount of B, however, was also found in the ionomer films tested in KOH. We infer that the B observed by XPS in the ionomer films is due to the presence of the contaminants in the supporting electrolyte, not additional B species entering the films.

The summary of the peak fitting and binding energies for Aemion, Sustainion, and PiperION is shown in Table S3. Complex polymer matrices such as ionomer films are challenging to analyze by XPS given that the peak positions are influenced by the bonding as well as the surrounding environment, which in an ionomer includes charged counterions. Using the published chemical structures, we tentatively identified the peaks composing C 1s and N 1s spectra (see below). Figure 3 shows the predicted chemical degradation routes for Aemion,[6,21,32] Sustainion,[3,5,33] and PiperION[6] polymers. A possible electrochemical route is shown for PiperION. However, all three polymers can degrade under applied potential through a variety of mechanisms.[15,16,19,34]

https://doi.org/10.1021/acsami.1c22472
ACS Appl. Mater. Interfaces 2022, 14, 18261−18274

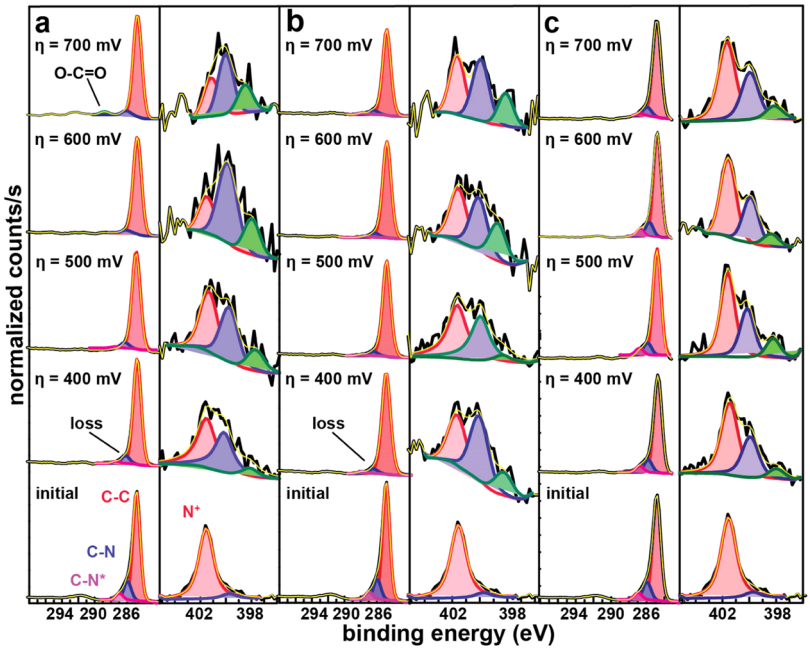

Figure 5. Changes to the chemical structure of Sustainion under applied potential. C 1s and N 1s XP spectra of Sustainion thin films tested at increasing overpotential in (a) pH 10, 1 M K_2CO_3/$KHCO_3$ buffer, (b) pH 14, 1 M KOH, and (c) pH 8, 1 M borate buffer.

3.2.1. Aemion Structural Changes. Aemion is composed of substituted phenyl and benzimidazole fragments (Figure 1a) and analyzed as a pristine thin film that has three peaks contributing to its C 1s spectrum (Figure 4, bottom panel). We assigned the peak at 284.8 eV to the C═C and C−H bonds that are dominant in that structure. The two smaller peaks at higher binding energies amount to about 20% of the total carbon in the structure and were assigned to C bound to N^+ and N. The N/C ratio based on the chemical structure and XPS data is ∼10 atom %. The N 1s spectrum of the pristine film was also fitted with three peaks. The peak at 401.4 eV was assigned to the N carrying the positive charge. The smaller peaks at 398.3 and 400 eV likely originate from other nitrogen atoms in the polymer structure that do not carry the positive charge.

The structural changes of the Aemion film after polarization in 1 M K_2CO_3/$KHCO_3$ buffer are shown in Figure 4a. At η = 400 mV, the film maintained its initial composition. At η = 500 mV, the Pt/C ratio, which allows us to track dissolution, increased from ∼0.11 to 0.28, though no new peaks appear in the XP spectra. At η = 600 mV, the film dissolution became more significant (Pt/C >1.0). A new peak at 288.2 eV appeared in the C 1s spectrum. The N 1s spectrum changes along with C 1s. The loss of the peak assigned to N^+ at 401.4 eV was observed. The N/C ratio increased from ∼0.10−0.11 to 0.17. The unchanged N/C ratio in the XP spectra prior to η = 600 mV suggests that during film degradation and consequent dissolution, both N and C are lost together. As the overpotential increases to 700 mV (the overpotential at which the film falls off the electrode), another carbon peak appears at 288.8 V, while N 1s completely lost its initial shape and settled at ∼399.1 eV. Thus, the hypothesis that the Aemion film suffers degradation in the K_2CO_3/$KHCO_3$ buffer and is lost from the electrode due to dissolution in the electrolyte appears supported by the XPS data.

Aemion exhibited a slight mass loss in 1 M KOH starting at η = 500 mV (Pt/C gradually increased from 0.11 to 0.26 between η = 500 and 700 mV). The N/C ratio remained constant as did the C−N/total-C ratio. The shape of the N 1s peak, however, changed; the contribution of the N^+ becomes smaller, while the other two N 1s peaks increase in relative intensity (Figure 4b). The changes of the N 1s peak in the absence of observed loss of nitrogen might indicate that some benzimidazole groups are demethylated or the N^+ is quenched through another mechanism. We do not see the appearance of any C 1s or N 1s peaks at higher binding energies than the original peaks as we observe in the K_2CO_3/$KHCO_3$ buffer. Thus, we did not observe any signs of polymer oxidation in KOH. The film loss during electrochemical testing in KOH is not as pronounced as in K_2CO_3/$KHCO_3$, suggesting that the ionomer is more stable in KOH.

In pH 8, 1 M borate buffer (Figure 4c), Aemion films demonstrated fewer changes to the film composition than in KOH. The N/C and C−N/total-C ratios remained constant throughout the electrochemical testing. The Pt/C counts slightly increased at η = 700 mV, which is likely due to ionomer instability at that overpotential independent of the electrolyte. However, the shape of the N 1s peak changed; diminished contribution from N^+ and increased contributions of the N 1s peaks at lower binding energies were observed.

The Aemion ionomer appears to undergo some structural changes along with dissolution in all three electrolytes but it appears to severely degrade only in the K_2CO_3/$KHCO_3$ buffer. The chemical degradation route predicted for Aemion through the OH^- nucleophilic attack is shown in Figure 3a.[21] The benzimidazolium ring opening and the formation of a carboxylate from the original polymer would lead to the film dissolution. Stabilized by a high degree of methylation, Aemion degrades through this mechanism only when OH^- becomes strongly nucleophilic, which might be induced by proximity to a charged electrode withdrawing electron density. Another possible degradation route is oxidation of the polymer structure by the OER intermediates or phenyl oxidation at the metal surface. Interestingly, the presence of carbonate/

https://doi.org/10.1021/acsami.1c22472
ACS Appl. Mater. Interfaces 2022, 14, 18261−18274

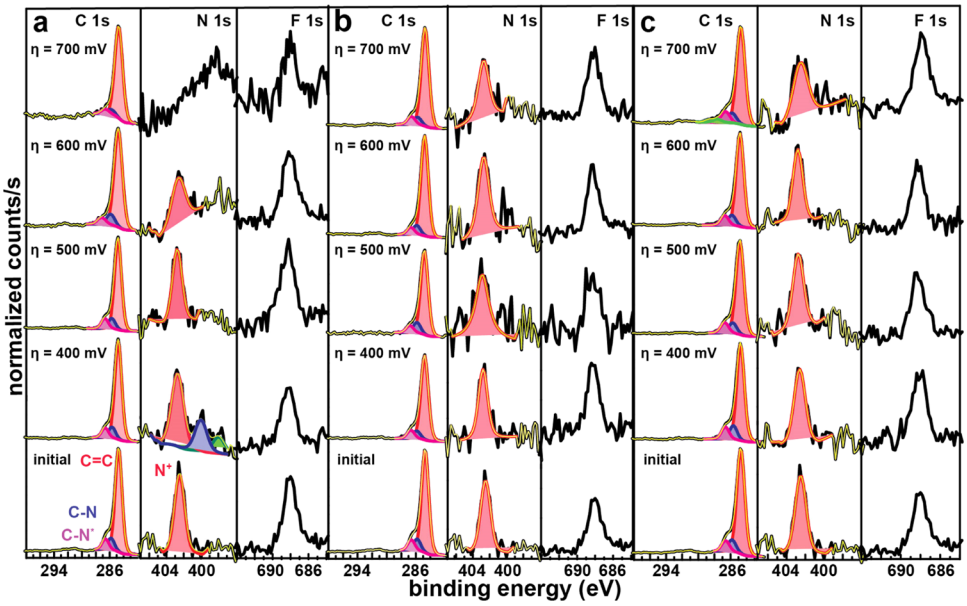

Figure 6. Changes to the chemical structure of PiperION under applied potential. C 1s, N 1s, and F 1s spectra for PiperION thin ionomer films tested in (a) pH 10, 1 M K_2CO_3/$KHCO_3$ buffer, (b) 1 M KOH, and (c) pH 8, 1 M borate buffer.

bicarbonate anions that are expected to interact with the ionomer strongly affects the stability of the film. The absence of the same degree of degradation in borate buffer (pH 8) compared to that of carbonate/bicarbonate buffer (pH 10) suggests that the pH of the bulk electrolyte alone does not dictate the stability. The complete loss of the film during the QCM experiment and the new higher-energy peaks in the C 1s spectrum point to the polymer backbone fracturing into soluble fragments leading to the film dissolution. Conductivity of Aemion in carbonate and bicarbonate solutions is significantly lower than in KOH (in 1 M $KHCO_3$, σ = 3.8 $mS{\cdot}cm^{-1}$; in 1 M K_2CO_3, σ = 2.0 $mS{\cdot}cm^{-1}$; in 1 M KOH, σ = 10.0 $mS{\cdot}cm^{-1}$ at room temperature).[21] Kiessling et al. demonstrated that membrane conductivity is especially important at high current densities.[35] We achieve higher current densities at higher overpotentials where Aemion shows signs of degradation. A concentration gradient along with a pH gradient might develop at the ionomer/bulk electrolyte interface, making the polymer more prone to oxidation due to either the local pH drop or the absence of OH^- to participate in OER.

3.2.2. Sustainion Structural Changes. The spectrum of C 1s for the pristine Sustainion film was fitted with three component peaks; the peak at 284.8 V originating from the C−C, C−H, and C═C in the structure and two peaks at 285.9 and 286.9 eV, which we again assigned to C bonded to N and N^+ (C bonded to N was ∼20% of the total carbon content) (Figure 5). The N 1s spectrum of the pristine film has two peaks; the dominant peak at 401.6 eV that corresponds to the N carrying the positive charge (the N in the imidazolium ring is chemically equivalent due to resonance) and a much smaller peak at 399.7 eV that was assigned to the N in the imidazolium ring that was insufficiently methylated. The N/C ratio for Sustainion thin film before testing was ∼6%.

Figure 5 shows similar changes occurring in the structure of Sustainion in pH 14 KOH and K_2CO_3/$KHCO_3$ buffer. The peaks in the C 1s spectrum assigned to C bonded to N diminished in both electrolytes (C−N/total-C ratio went down from 20 to 5−9% in both electrolytes as early in the testing as at η = 400 mV) and shifted by ∼0.5 eV. The N/C ratio went from 6% to 3% indicating N loss. The N 1s peak shape changed under applied potential in a similar way in both supporting electrolytes. The peak at 401.5 eV assigned to N^+ no longer dominates. Even at the lowest overpotential (η = 400 mV) in both supporting electrolytes, we now observed a set of three peaks more comparable in size at 401.6, 399.9, and 398.1 eV. However, the N^+ peak is not completely lost. The Pt/C ratio increases slightly by η = 600 mV in both electrolytes pointing at a small portion of the film dissolving.

Figure 5c shows the changes to the C 1s and N 1s XP spectra of Sustainion tested in 1 M borate buffer at pH 8. The C−N/total-C ratio decreased from 20 to 16%, which is a smaller change than in KOH or K_2CO_3/$KHCO_3$ where the C−N/total-C ratio decreased by >50%. The N/C and Pt/C ratios remained unchanged. The N 1s peak underwent changes similar to those we observed in KOH and K_2CO_3/$KHCO_3$, but in this electrolyte, the N^+ peak remained dominant.

Two of the possible chemical degradation routes for Sustainion are shown in Figure 3b. Imidazolium ring opening can be promoted by a nucleophilic attack.[36] The decrease in the C−N/total-C ratio along with the material dissolution seen in the XPS results appears consistent with the loss of the imidazolium side chains. The loss of side chains, but not the backbone, is consistent with the ionomer film remaining on the electrode during QCM testing. However, N is still present in the film and, based on the new N 1s peaks at lower binding energy, is experiencing changes in its oxidation state or bonding environment. This would be possible if the imidazolium was undergoing structural changes prior to the complete degradation and separation from the backbone. Thus, ring opening might be an intermediate to the removal of the imidazole group or routes 1 and 2 might occur concurrently in the case of chemical degradation by nucleophilic attack. However, Sustainion does not obviously degrade in the supporting electrolytes chosen for this study without applied potential. Thus, if a nucleophilic attack is occurring, it appears facilitated in some way by the oxidizing potential.

https://doi.org/10.1021/acsami.1c22472
ACS Appl. Mater. Interfaces 2022, 14, 18261−18274

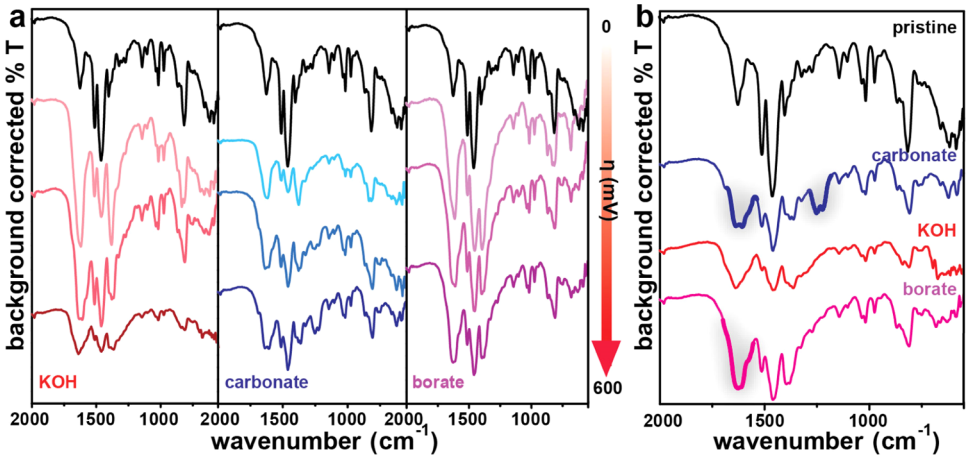

Figure 7. Chemical changes in the structure of Aemion probed by ATR-FTIR. (a) ATR-FTIR spectra of Aemion films collected after testing the films in 1.0 M KOH (red traces), 1 M K_2CO_3/$KHCO_3$ buffer pH 10 (blue traces), and 1 M borate buffer pH 8 (purple traces). Top to bottom: the black trace is of the pristine Aemion film and then in order of increasing overpotential (η = 400, 500, and 600 mV). (b) ATR-FTIR spectra collected on Aemion films tested at η = 600 mV in the three supporting electrolytes.

Electrochemical degradation pathways are also possible. For instance, the phenyl connecting the imidazole ring to the backbone might be oxidized by OER intermediates or at the metal surface leading to the loss of the charge-carrying group. Unlike Aemion, Sustainion degraded the least in the electrolyte with the lowest pH while having an almost identical degree of structural changes in KOH and carbonate/bicarbonate buffer. Sustainion does not seem to be affected specifically by the interactions with CO_3^{2-}/HCO_3^- anions as it degrades to the same extent in KOH. Perhaps, the origin of Sustainion's tolerance of CO_3^{2-}/HCO_3^- anions is its ability to conduct these anions more efficiently than Aemion. The conductivity reported for Sustainion-X24 membrane in 1 M $KHCO_3$ is 24 mS·cm^{-1} at room temperature, which is considerably lower than its conductivity in 1 M KOH (64 mS·cm^{-1})[37] but still much higher than the conductivity of Aemion in CO_3^{2-}/HCO_3^- forms (in 1 M $KHCO_3$, σ = 3.8 mS·cm^{-1}; in 1 M K_2CO_3, σ = 2.0 mS·cm^{-1}). The least degradation in the lowest pH might be indicative of Sustainion being more affected by the concentration of OH^- in the electrolytes and undergoing the loss of side chains as a result of the nucleophilic attack or an oxidation reaction involving OH^- attack and electron transfer.

3.2.3. PiperION Structural Changes. We then examined if PiperION thin films show signs of oxidative damage in the supporting electrolytes under applied potential. In addition to looking at C 1s and N 1s spectra, we also collected F 1s spectra to monitor the trifluoromethyl group stability during operation (the F/C ratio in the pristine film was calculated to be ∼1−2%). The C 1s spectrum was fitted with three peaks: the dominant peak at 284.8 eV assigned to C−C, C−H, and C═C and two smaller peaks at 285.9 and 286.7 eV for C−N^+ bonds (Figure 6, bottom panel). The N 1s peak for PiperION was fitted with only one peak at 402.7 eV and was assigned to the N^+ present in the structure in the piperidinium ring (N/C is about 3−4% in the pristine film, and ∼18% of C is bonded to N out of the total carbon content).

In K_2CO_3/$KHCO_3$, the film dissolution was observed at lower overpotentials (Figure 6a). At η = 400 mV, the N 1s spectrum changes to include several peaks at lower binding energy but the new N 1s peaks disappear by η = 500 mV. The observed changes to the shape of the N 1s peak might originate from the intermediates of the degradation process. By η = 600 mV, the Pt/C ratio went from 11 to 41% along with a small decrease in the N/C and C−N/total-C ratios. As the overpotential of 700 mV was reached, the dissolution became more significant (Pt/C = 150%) with N 1s peak shifting to lower binding energy and decreasing in intensity. The amount of C bonded to N also decreased by half. The F/C ratio for η = 600 and 700 mV was 4 and 3%, respectively (compared to 1−2% in the pristine ionomer film), suggesting that while the trifluoromethyl group remains, other carbon-containing fragments are lost. However, we do not see any sign of carbon-forming new bonds characteristic of degradation products. The decrease in the N content and the absence of a more pronounced mass loss during the QCM test are suggestive of the chemical changes occurring at the charge-carrying side chains. It is, nonetheless, difficult to pinpoint the mechanism of degradation. The degradation products could dissolve in the supporting electrolyte and thus not be picked up by the XPS analysis.

During the electrochemical testing in 1.0 M KOH, PiperION film was not observed to dissolve/detach until η = 700 mV (Figure 6b). At η = 700 mV, the Pt/C ratio increased but not significantly: from 11 to 16%. The C−N/total-C ratio decreased, and the F/C ratio increased.

In borate buffer (Figure 6c), despite a lower pH, no changes in the film structure were observed until η = 700 mV. We suspect that PiperION is not stable at this overpotential, and this degradation is independent of electrolyte identity. By the end of the electrochemical testing, the Pt/C ratio went from 11 to 30%.

PiperION was not observed to dissolve or sustain chemical changes in 1.0 M KOH and pH 8 borate buffer until η = 700 mV. Thus, it does not seem to be affected by a high or low concentration of OH^- in the supporting electrolyte. However, in K_2CO_3/$KHCO_3$ buffer, the polymer underwent chemical changes and dissolved. One of the possible electrochemical degradation routes for this polymer is the oxidation of the phenyl ring in the backbone (Figure 3c). However, we were not able to observe any degradation products consistent with that mechanism. Another mechanism might take place or the degradation products may dissolve into the electrolyte making it difficult to track them. To try and pinpoint the possible

https://doi.org/10.1021/acsami.1c22472
ACS Appl. Mater. Interfaces 2022, 14, 18261−18274

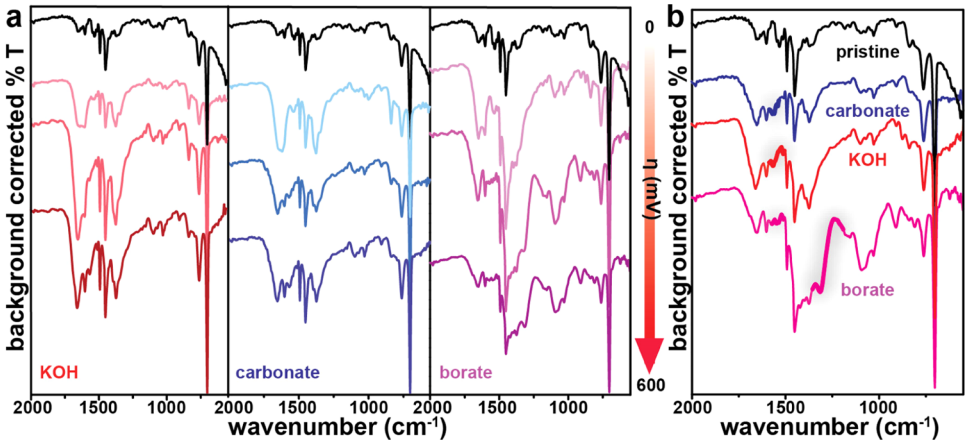

Figure 8. Chemical changes in the structure of Sustainion probed by ATR-FTIR. (a) ATR-FTIR spectra of Sustainion films collected after testing the films in 1.0 M KOH (red traces), 1 M K_2CO_3/$KHCO_3$ buffer pH 10 (blue traces), and 1 M borate buffer pH 8 (purple traces). Top to bottom: the black trace is of the pristine Sustainion film and then in order of increasing overpotential (η = 400, 500, and 600 mV). (b) ATR-FTIR spectra collected on Sustainion films tested at η = 600 mV in the three supporting electrolytes.

reasons for the instability of PiperION in carbonate/bicarbonate buffer specifically, we considered the conductivity of PiperION in carbonate and bicarbonate electrolytes. The conductivity of the PiperION solid membrane in water at room temperature when it is ion-exchanged to the carbonate form is 6 mS·cm^{-1}, and 5 mS·cm^{-1} when it is ion-exchanged to the bicarbonate form.[38] These values are higher than the conductivity of Aemion in carbonate/bicarbonate electrolytes but significantly lower than the carbonate/bicarbonate conductivity reported for Sustainion. However, the conductivities reported in the literature are affected by the measurement method. For example, in the recent work by Endrődi et al., the conductivities of PiperION and Sustainion in carbonate and bicarbonate electrolytes were measured for a range of elevated temperatures and were found comparable.[39] PiperION might be affected by a lower local pH due to the concentration and pH gradients forming at the interface of the thin film and bulk electrolyte or be subjected to oxidation by the electrode surface in the absence of OH^- due to the low conductivity of CO_3^{2-}/HCO_3^- anions.

3.3. Attenuated Total Reflectance (ATR) FTIR Spectroscopy Analysis of the Ionomer Films after Electrochemical Testing. To further investigate the film degradation processes in the presence of the electrolytes under applied potential, we employed ATR-FTIR on 5 wt % ionomer films.

3.3.1. Aemion ATR-FTIR Analysis. The summary of the changes in the Aemion spectrum under each applied potential in the three electrolytes is shown in Figure 7. In the pristine film (black traces in Figure 7), the vibrational mode at 1630 cm^{-1} was assigned to the C═N bond in the imidazole fragment. We find a similar mode in the spectrum of an imidazole compound in the literature.[40,41] The most noticeable changes in the spectrum occurred in the K_2CO_3/$KHCO_3$ buffer. The mode at 1630 cm^{-1} transformed into two vibrational modes with maxima at 1640 and 1610 cm^{-1}. At η = 500 mV, two new modes appeared at 1250 and 1220 cm^{-1}; the mode at 1400 cm^{-1} transformed into multiple modes, and a small vibrational mode appeared at 753 cm^{-1}. The transformation of the C═N mode into multiple modes can be interpreted as the loss of the imidazole ring and possible formation of N−H and other C═C bonds in the changed structure. The new modes at 1250 and 1220 cm^{-1} can originate from a C−N or a C−O bond formation.

The changes observed by ATR-FTIR for Aemion tested in KOH are not as pronounced (Figure 7, red traces). The vibrational mode at 1400 cm^{-1} converts into multiple modes, similarly to the changes we observe in the K_2CO_3/$KHCO_3$ buffer. The small modes in the 1300−1250 cm^{-1} range disappear but do not convert into new modes that appeared in K_2CO_3/$KHCO_3$. A small mode appears at 753 cm^{-1} at η = 500 mV, which is the region that describes changes in substitution in aromatic compounds. This may indicate a demethylation of the nitrogen in the imidazole as a result of the OH^- attack or a different mechanism. The 500 mV is the same overpotential at which we start observing film loss and diminishing C−N/total-C ratio by XPS.

Figure 7 also shows the gradual changes in the film structure in a 1 M borate buffer. The vibrational mode at 1630 cm^{-1} deforms slightly compared to its initial shape and the region between 1400 and 1250 cm^{-1} changes. The mode at 1390 cm^{-1} turns into two modes, and the small modes at ∼1320 cm^{-1} disappear. The observed changes might be indicative of changes to the N bonding environment. However, the changes are not significant enough to cause film loss that would be apparent by QCM and XPS.

ATR-FTIR data for Aemion is consistent with the XPS results: it shows that the film undergoes some structural changes in every supporting electrolyte, with the changes in the carbonate/bicarbonate buffer being the most significant. The XPS analysis of the film tested in the carbonate/bicarbonate buffer shows the formation of C═O species along with N^+ loss and film dissolution. ATR-FTIR confirms these changes showing the loss of the C═N mode intensity and several other new modes growing.

3.3.2. Sustainion ATR-FTIR Analysis. Sustainion ATR-FTIR spectra at different overpotentials were collected in a similar manner (Figure 8). Like Aemion, Sustainion possesses an imidazole group. We assigned the vibrational mode at 1650 cm^{-1} to the C═N in imidazole. The spectrum of Sustainion undergoes similar transformations after electrochemistry in KOH and K_2CO_3/$KHCO_3$ buffer, with both the 1650−1530 and 1370−1330 cm^{-1} regions changing. We observed the shape transformation of the mode assigned to imidazole, the

https://doi.org/10.1021/acsami.1c22472
ACS Appl. Mater. Interfaces 2022, 14, 18261−18274

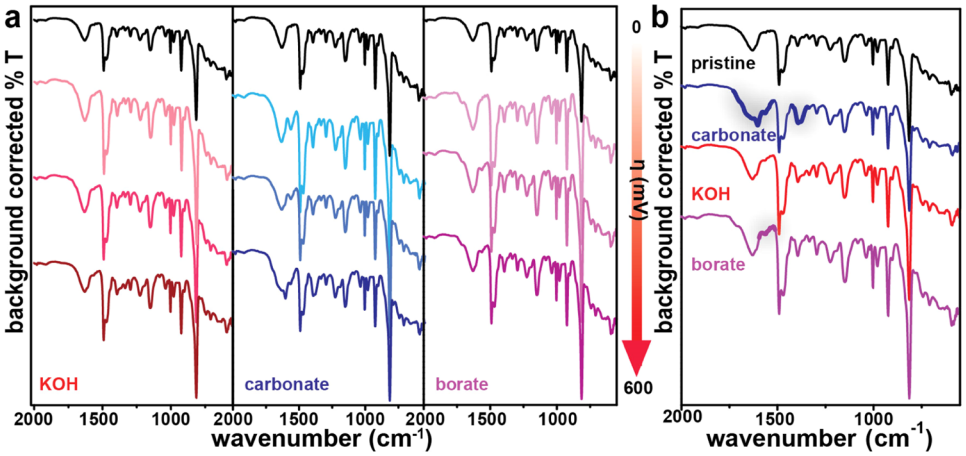

Figure 9. Chemical changes in the structure of PiperION probed by ATR-FTIR on a diamond crystal. (a) ATR-FTIR spectra of PiperION films collected after testing the films in 1.0 M KOH (red traces), 1 M K_2CO_3/$KHCO_3$ buffer pH 10 (blue traces), and 1 M borate buffer pH 8 (purple traces). Top to bottom: the black trace is of the pristine PiperION film and then in order of increasing overpotential (η = 400, 500, and 600 mV). (b) ATR-FTIR spectra collected on PiperION films tested at η = 600 mV in the three supporting electrolytes.

loss of the vibrational mode at 1533 cm^{-1}, and the growth of a mode at 1567 cm^{-1}. This region of the spectrum can have modes from a variety of bonds including C═N, C═O, and O−N═O. The mode in the 1370−1330 cm^{-1} region changes from a small broad one to a sharp mode. The observed changes in the spectrum of Sustainion might originate from transformations of the imidazole ring, leading to its loss due to the nucleophilic OH^- attack or by electrochemical oxidation. Pellerite et al. reported similar changes in the IR spectrum of Sustainion soaked in 1 M KOH for 24 h without any applied potential.[36] In that case, the observed changes in the spectrum were later reversed by a soak in 1 N HCl and were attributed to the formation of a carboxylated zwitterion upon CO_2 addition, not permanent degradation by the ring opening.[36] We, however, do not believe that Sustainion under applied potential undergoes reversible changes in the KOH or carbonate/bicarbonate buffer given the loss of nitrogen and C−N bonds observed by XPS. The ionomer films tested in the borate buffer show fewer changes in the spectrum. The 1533 cm^{-1} mode disappears, but no new mode appears at 1567 cm^{-1}. There is a new vibrational mode at 1313 and 813 cm^{-1}. The mode at 1313 cm^{-1} might originate from the borate species present in the film, but given the low amount of boron determined by XPS, we conclude this is unlikely.

These studies suggest that Sustainion is sensitive of the basicity of the electrolyte but might not be strongly affected by anions such as CO_3^{2-} or HCO_3^-. XPS showed considerable loss of the C−N bonds in both KOH and carbonate/bicarbonate buffer. ATR-FTIR data supports these results showing changes in the C═N imidazole mode that suggest that the charge-carrying group is degrading. This process might be unaffected by the presence of CO_3^{2-} or HCO_3^- due to the high carbonate/bicarbonate conductivity reported for Sustainion. Fast conduction of the anions through the ionomer film during operation would facilitate the transfer of OH^- (and protons in the form of HCO_3^-) to (and away from) the electrode surface. These processes would decrease the pH gradient and provide sufficient OER reactants to avoid ionomer oxidation.

3.3.3. PiperION ATR-FTIR Analysis. The ATR-FTIR spectra of PiperION after electrochemistry in the three electrolytes are shown in Figure 9. Consistent with our XPS results, the most noticeable changes in the ATR-FTIR spectrum of PiperION are observed in the K_2CO_3/$KHCO_3$ buffer (Figure 9, blue traces). The vibrational mode at 1630 cm^{-1} transforms into multiple modes at 1640, 1605, and 1558 cm^{-1}. The mode at 1558 cm^{-1} appears at η = 400 mV, and the one at 1605 cm^{-1} appears at η = 600 mV. The mode at 1395 cm^{-1} converts into two modes by η = 600 mV. We, however, did not observe the appearance of a stretch or a bend consistent with a carboxylate formation, which is a degradation product predicted by the electrochemical oxidation route. The changes in the 1640−1560 cm^{-1} region of the spectrum might result from the formation of new C═N or C═C bonds.

The PiperION film tested in KOH does not seem to undergo any structural changes as no new vibrational modes appeared in the ATR-FTIR spectrum. We also did not observe any chemical changes in KOH by XPS (except at η = 700 mV). The ATR-FTIR spectra of the film tested in borate buffer have a small change in the 1600−1500 cm^{-1} region: a new mode appears at 1558 cm^{-1}, similarly to that observed in the K_2CO_3/$KHCO_3$ buffer. The mode becomes noticeable at η = 500 mV and might be the result of some changes in the structure of the ionomer.

PiperION did not show any signs of significant structural changes in KOH or borate buffer evident by QCM, XPS (until η = 700 mV), and ATR-FTIR. The stability of the ionomer, however, can be impacted by the presence of a metal oxide catalyst undergoing OER in an electrolyzer. We showed that PiperION ionomer in direct contact with IrO_x powder at the anode of an AEMWE oxidizes substantially and loses headgroups.[14] In the carbonate/bicarbonate buffer, PiperION undergoes structural changes, as suggested by our XPS and ATR-FTIR data. XPS showed N loss and film dissolution but without new peaks appearing in the C 1s spectra. ATR-FTIR spectra revealed several new modes growing and the existing modes changing shape. Based on the evidence presented by the surface characterization techniques, the polymer undergoes dissolution (e.g., we find an increase in the Pt/C ratio by XPS after electrochemistry). We, however, cannot be sure in the (electro)chemical mechanism because some of the degradation products might dissolve into the electrolyte and avoid detection.

https://doi.org/10.1021/acsami.1c22472
ACS Appl. Mater. Interfaces 2022, 14, 18261−18274

3.4. Computational Studies of Ionomer Oxidative Stability. To help differentiate between chemical and electrochemical degradation routes for these polymers, we performed DFT calculations to computationally examine redox potentials (E_0) of the polymer structures and to predict where the oxidation is likely to occur within the polymer. The predicted E_0 of the polymers suggests which are more likely to oxidize under applied potential. The identification of the chemical functionality of the polymer that the E_0 corresponds to leads to a better understanding of the degradation pathway(s).

Our calculations indicate that E_0 for the ionomers are Sustainion (2.18 eV vs SHE *cis*, 2.33 eV vs SHE *trans*) > PiperION (1.78 eV vs SHE) > Aemion (1.46 eV vs SHE) (Figure 10). The range of values for Sustainion is attributed to

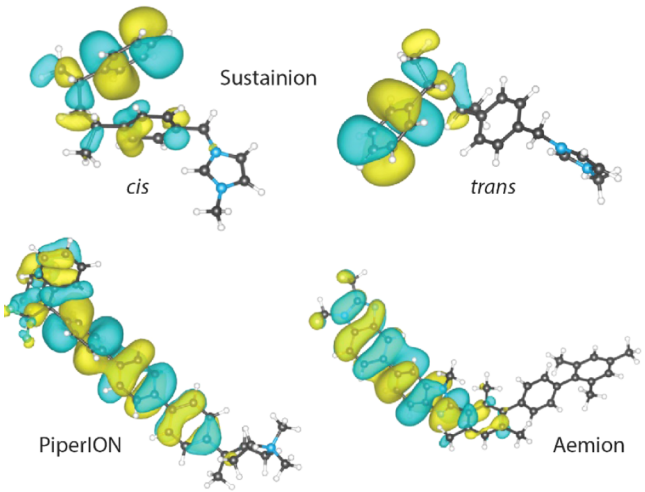

Figure 10. HOMO electronic occupation diagram calculated by DFT for the ionomer fragments indicated. The HOMO is, to a first approximation, the energetically most favorable site for oxidation to occur.

the competing effects produced by π-stacking: the destabilization of the ground state and the stabilization of the spin density via a multicenter single-electron bond. The latter was observed for the imidazolium-containing side chain. Given the stabilization provided by the imidazole fragment, the phenyl ring in contact with it is less likely to be oxidized than the phenyl ring next to it without the charge-carrying group. However, the E_0 for this route is very high. The experimental data shows changes in the N 1s bonding environment or oxidation state, which would not occur in the case of phenyl oxidation. A possible route for Sustainion degradation, given a high E_0 for phenyl oxidation, is the loss of the side chains through the OH^- attack on the C connecting the phenyl and imidazole fragment or the imidazole ring leading to the loss of the side chains. This mechanism is perhaps promoted by the applied potential as we see no evidence of Sustainion degrading in the supporting electrolytes without applied potential.

Within the PiperION structure, the phenyl rings adjacent to the trifluoromethyl group help stabilize the HOMO by withdrawing electron density, which decreases electron−electron repulsion. Oxidative attack is thus likely to affect the other phenyl rings in the backbone that are occupied by higher-energy electrons. The changes we observed experimentally are more consistent with the attack on the charge-carrying groups given the changes in the shape of the N 1s spectrum and the absence of carboxylate-related C 1s peaks or vibrational modes. However, that does not rule out the electrochemical aromatic oxidation as degradation products may be in small amounts and/or dissolve into the electrolyte.

Because Aemion has the lowest E_0, it appears most likely to suffer from oxidative damage. Our calculations suggest that oxidizing any cationic motif is unlikely. The E_0 corresponds to the removal of an electron from the benzimidazole. The likeliest point of oxidative damage is the N in the benzimidazole that does not have a methyl group attached to it (Figure 1a). The methyl groups on the substituted phenyl and imidazolium rings add spin stabilization. The imidazolium ring opening is also proposed as the chemical degradation route. We suspect that the polymer degrades through cleavage of the imidazole ring, with applied potential playing a role in the process. Aemion does not degrade in 1.0 M KOH without applied potential, nor does it degrade in carbonate/bicarbonate solutions. Thus, the routes leading to the polymer damage might include an OH^- attack on the polarized bonds or a direct oxidation of the structure by the OER intermediates or the electrode surface.

3.5. Analyzing the Ionomer Stability in Acidic Environment. The higher degree of structural changes that Aemion and PiperION showed in 1 M carbonate/bicarbonate buffer compared to that of the other electrolytes suggested that the interactions of the HCO_3^-/CO_3^{2-} anions with the ionomer matrices play a role in the stability of the polymers during OER. Our two hypotheses in regard to the effect anions have on the ionomer were (i) the development of a pH gradient with consecutive ionomer oxidation facilitated by a local pH drop at the electrode surface and/or (ii) poor transport of OH^- to the electrode surface due to low carbonate/bicarbonate conductivity of Aemion and PiperION, which leads to the ionomer oxidation reaction dominating. To determine if the low pH in addition to the applied potential was responsible for the observed structural changes, we tested the thin 0.16 wt % ionomer films in 0.1 M $HClO_4$ (pH ~1) at η = 400 and 600 mV and analyzed them with XPS.

The stability of Aemion in the acidic environment seems to be better than in the carbonate/bicarbonate buffer (Figure S6a shows XPS data and fitting). No film dissolution or appearance of new C or N peaks was observed at η = 400 mV. At η = 600 mV, while no changes in the C 1s and N 1s were observed, the Pt/C ratio from XPS slightly increased signifying film dissolution. Aemion does not appear to be affected by the acidic pH while under applied potential and, thus, is likely not degrading in the carbonate/bicarbonate buffer due to the local pH drop. Given that we observed some degree of dissolution in all four tested electrolytes, we hypothesize that ionomer oxidation facilitated by applied potential occurs in all cases but at a different rate. Testing Aemion in pH 1 acid showed its good stability in acidic conditions. Thus, we were left to suggest that the difference in OH^- vs CO_3^{2-}/HCO_3^- conductivities is causing Aemion to degrade in carbonate, perhaps due to the formation of a modest pH gradient and lack of OH^- to oxidize at the electrode surface.

The structural changes observed for Sustainion tested in acid resemble the results of the electrochemical testing in borate buffer (Figure S6b). At η = 400 mV, no dissolution was observed, but there was a small loss of the C−N bonds and a change in the shape of the N 1s peak. At η = 600 mV, film dissolution was identified and the loss of C−N bonds became

https://doi.org/10.1021/acsami.1c22472
ACS Appl. Mater. Interfaces 2022, 14, 18261−18274

more pronounced. However, the N 1s peak assigned to N^+ still dominated the spectra for all overpotentials. Sustainion sustained less damage in the acidic environment than in base. Sustainion was apparently designed to operate in the carbonate-containing environment. It degraded the most in the electrolytes of higher basicity but only when potential was applied. Given the comparably higher E_0 estimated from DFT, we hypothesize that the OH^- attack becomes more likely when the film is polarized by the electrode surface. It seems likely that the carbonate/bicarbonate conductivity of Sustainion is high enough to perhaps suppress larger pH gradients.

Interestingly, PiperION sustained significant damage in 0.1 M $HClO_4$ (Figure S6c). At η = 400 mV, no dissolution was observed, but a new high-energy peak appeared in the N 1s spectrum. At η = 600 mV, the F/C ratio doubled, and the Pt/C ratio increased signifying film dissolution. N 1s peak remained at the same binding energy as in the pristine film but decreased in intensity. The C 1s spectrum gained several peaks at higher binding energy pointing to the formation of new C compounds. The amount of the film loss during electrochemical testing in acid is similar to the film loss observed in the carbonate/bicarbonate buffer. Thus, for PiperION, we hypothesize that its stability might depend on both the carbonate/bicarbonate conductivity and the local pH drop, as we see degradation occurring in both $HClO_4$ and carbonate/bicarbonate buffer. We also know from our previous work that PiperION is subject to oxidative degradation when used for a prolonged operation in pure water AEMWE with IrO_x and that pH gradients are likely at high current densities.[14]

4. CONCLUSIONS

We analyzed the effects of supporting electrolytes on the stability of anion-conducting ionomers under oxidizing potentials in the context of their application in alkaline membrane electrolyzers. The ionomers demonstrated different degrees of stability in KOH, K_2CO_3/$KHCO_3$ buffer, borate buffer, and $HClO_4$. Aemion degraded and dissolved in all four electrolytes, with damage to the chemical structure being the most pronounced in the carbonate/bicarbonate buffer. The stability of Aemion seems to be affected by strongly interacting carbonate/bicarbonate anions that may prevent a rapid flux of OH^- to the electrode surface and allow ionomer oxidation. PiperION showed material loss in the carbonate/bicarbonate buffer and acidic conditions, remaining stable in KOH and borate buffer. The low conductivity of carbonate/bicarbonate forms of PiperION might facilitate a pH gradient leading to oxidative changes in the polymer due to the local pH drop or the absence of sufficient OH^- for OER in which case the relative polymer oxidation rate increases. Sustainion exhibited the same degree of degradation in KOH and carbonate/bicarbonate buffer and little observed degradation in borate buffer and $HClO_4$. The degradation for this ionomer appears to be triggered primarily by the applied potential but seems to be favored in electrolytes with higher OH^- concentration. We also acknowledge that the presence of OER catalysts can introduce additional degradation pathways (Figure S7).[14]

Looking forward, gas chromatography coupled with mass spectrometry and nuclear magnetic resonance spectroscopy can be employed to analyze (dilute) soluble ionomer fragments to unravel the mechanisms of ionomer degradation. The analysis of postmortem GDLs from pure-water-fed AEMWE will also be key, as shown by our initial results.[14]

In sum, we demonstrated that a combination of characterization techniques can unravel some of the processes at the ionomer/catalyst interface. The three-electrode setup was a simple model system that mimics in many ways the anode of the AEMWE. This approach can be successfully employed to test the interactions of a variety of OER catalysts (PGM and non-PGM). Such experiments can be run in parallel with the AEMWE tests (with the GDLs being analyzed as well) to gain a comprehensive understanding of water electrolysis in a zero-gap configuration.

■ ASSOCIATED CONTENT

Supporting Information

The Supporting Information is available free of charge at https://pubs.acs.org/doi/10.1021/acsami.1c22472.

Calculated thicknesses of ionomer films; hydration energies of the anions in the supporting electrolytes; XPS fitting of C 1s, N 1s, and F 1s peaks of ionomer films tested in supporting electrolytes; additional material processing details; ionomer stability under XPS beam; stability of Aemion and Sustainion films after alternative preconditioning; stability of PiperION films after alternative preconditioning in carbonate buffer; and XPS spectra of the three ionomers tested in $HClO_4$ (PDF)

■ AUTHOR INFORMATION

Corresponding Author

Shannon W. Boettcher − *Department of Chemistry and Biochemistry and Materials Science Institute, University of Oregon, Eugene, Oregon 97403, United States; Oregon Center for Electrochemistry, University of Oregon, Eugene, Oregon 97403, United States;* orcid.org/0000-0001-8971-9123; Email: swb@uoregon.edu

Authors

Raina A. Krivina − *Department of Chemistry and Biochemistry and Materials Science Institute, University of Oregon, Eugene, Oregon 97403, United States; Oregon Center for Electrochemistry, University of Oregon, Eugene, Oregon 97403, United States*

Grace A. Lindquist − *Department of Chemistry and Biochemistry and Materials Science Institute, University of Oregon, Eugene, Oregon 97403, United States; Oregon Center for Electrochemistry, University of Oregon, Eugene, Oregon 97403, United States*

Min Chieh Yang − *Department of Chemistry and Biochemistry and Materials Science Institute, University of Oregon, Eugene, Oregon 97403, United States; Oregon Center for Electrochemistry, University of Oregon, Eugene, Oregon 97403, United States*

Amanda K. Cook − *Department of Chemistry and Biochemistry and Materials Science Institute, University of Oregon, Eugene, Oregon 97403, United States;* orcid.org/0000-0003-3501-8502

Christopher H. Hendon − *Department of Chemistry and Biochemistry and Materials Science Institute, University of Oregon, Eugene, Oregon 97403, United States; Oregon Center for Electrochemistry, University of Oregon, Eugene, Oregon 97403, United States;* orcid.org/0000-0002-7132-768X

https://doi.org/10.1021/acsami.1c22472
ACS Appl. Mater. Interfaces 2022, 14, 18261−18274

Andrew R. Motz − *Nel Hydrogen, Wallingford, Connecticut 06492, United States*
Christopher Capuano − *Nel Hydrogen, Wallingford, Connecticut 06492, United States*
Katherine E. Ayers − *Nel Hydrogen, Wallingford, Connecticut 06492, United States*
James E. Hutchison − *Department of Chemistry and Biochemistry and Materials Science Institute, University of Oregon, Eugene, Oregon 97403, United States;* orcid.org/0000-0003-2605-3226

Complete contact information is available at: https://pubs.acs.org/10.1021/acsami.1c22472

Notes

The authors declare no competing financial interest.

■ ACKNOWLEDGMENTS

This work was supported by the U.S. Department of Energy's Office of Energy Efficiency and Renewable Energy (EERE) under the Fuel Cell Technologies Office (FCTO) under award DE-EE0008841. The authors acknowledge the UO CAMCOR Facility, supported by grants from the W.M. Keck Foundation, the M.J. Murdock Charitable Trust, ONAMI, the Air Force Research Laboratory (Agreement Number FA8650-05-1-5041), NSF (Award Numbers 0923577 and 0421086), and the University of Oregon. The authors thank S. Golledge for assistance with XPS and also S. Oener for the valuable discussion. Versogen is acknowledged for the valuable discussion on ionomer preconditioning.

■ REFERENCES

(1) Pivovar, B.; Rustagi, N.; Satyapal, S. Hydrogen at Scale (H_2@ Scale): Key to a Clean, Economic, and Sustainable Energy System. *Electrochem. Soc. Interface* **2018**, *27*, 47−52.
(2) Ayers, K.; Danilovic, N.; Ouimet, R.; Carmo, M.; Pivovar, B.; Bornstein, M. Perspectives on Low-Temperature Electrolysis and Potential for Renewable Hydrogen at Scale. *Annu. Rev. Chem. Biomol. Eng.* **2019**, *10*, 219−239.
(3) Yang, C.; Wang, S.; Ma, W.; Jiang, L.; Sun, G. Highly Alkaline Stable N1-alkyl Substituted 2-methylimidazolium Functionalized Alkaline Anion Exchange Membranes. *J. Mater. Chem.* **2015**, *3*, 8559−8565.
(4) Vincent, I.; Bessarabov, D. Low Cost Hydrogen Production by Anion Exchange Membrane Eelectrolysis: A Review. *Renew. Sust. Energ. Rev.* **2018**, *81*, 1690−1704.
(5) Mustain, W. E.; Chatenet, M.; Page, M.; Kim, Y. S. Durability Challenges of Anion Exchange Membrane Fuel Cells. *Energy Environ. Sci.* **2020**, *13*, 2805−2838.
(6) Li, D.; Motz, A. R.; Bae, C.; Fujimoto, C.; Yang, G.; Zhang, F.-Y.; Ayers, K. E.; Kim, Y. S. Durability of Anion Exchange Membrane Water Electrolyzers. *Energy Environ. Sci.* **2021**, *14*, 3393−3419.
(7) Li, D.; Park, E. J.; Zhu, W.; Shi, Q.; Zhou, Y.; Tian, H.; Lin, Y.; Serov, A.; Zulevi, B.; Baca, E. D.; Fujimoto, C.; Chung, H. T.; Kim, Y. S. Highly Quaternized Polystyrene Ionomers for High Performance Anion Exchange Membrane Water Electrolysers. *Nat. Energy* **2020**, *5*, 378−385.
(8) Xu, D.; Stevens, M. B.; Cosby, M. R.; Oener, S. Z.; Smith, A. M.; Enman, L. J.; Ayers, K. E.; Capuano, C. B.; Renner, J. N.; Danilovic, N.; Li, Y.; Wang, H.; Zhang, Q.; Boettcher, S. W. Earth-Abundant Oxygen Electrocatalysts for Alkaline Anion-Exchange-Membrane Water Electrolysis: Effects of Catalyst Conductivity and Comparison with Performance in Three-Electrode Cells. *ACS Catal.* **2019**, *9*, 7−15.
(9) Xiao, J.; Oliveira, A. M.; Wang, L.; Zhao, Y.; Wang, T.; Wang, J.; Setzler, B. P.; Yan, Y. Water-Fed Hydroxide Exchange Membrane Electrolyzer Enabled by a Fluoride-Incorporated Nickel−Iron Oxyhydroxide Oxygen Evolution Electrode. *ACS Catal.* **2021**, *11*, 264−270.
(10) Mališ, J.; Mazúr, P.; Paidar, M.; Bystron, T.; Bouzek, K. Nafion 117 Stability under Conditions of PEM Water Electrolysis at Elevated Temperature and Pressure. *Int. J. Hydrog. Energy* **2016**, *41*, 2177−2188.
(11) Miller, H. A.; Bouzek, K.; Hnat, J.; Loos, S.; Bernäcker, C. I.; Weißgärber, T.; Röntzsch, L.; Meier-Haack, J. Green Hydrogen from Anion Exchange Membrane Water Electrolysis: A Review of Recent Developments in Critical Materials and Operating Conditions. *Sustain. Energy Fuels* **2020**, *4*, 2114−2133.
(12) Stanislaw, L. N.; Gerhardt, M. R.; Weber, A. Z. Modeling Electrolyte Composition Effects on Anion-Exchange-Membrane Water Electrolyzer Performance. *ECS Trans.* **2019**, *92*, 767−779.
(13) Vincent, I.; Kruger, A.; Bessarabov, D. Development of Efficient Membrane Electrode Assembly for Low Cost Hydrogen Production by Anion Exchange Membrane Electrolysis. *Int. J. Hydrog. Energy* **2017**, *42*, 10752−10761.
(14) Lindquist, G. A.; Oener, S. Z.; Krivina, R.; Motz, A. R.; Keane, A.; Capuano, C.; Ayers, K. E.; Boettcher, S. W. Performance and Durability of Pure-Water-Fed Anion Exchange Membrane Electrolyzers Using Baseline Materials and Operation. *ACS Appl. Mater. Interfaces* **2021**, *13*, 51917−51924.
(15) Borup, R.; Meyers, J.; Pivovar, B.; Kim, Y. S.; Mukundan, R.; Garland, N.; Myers, D.; Wilson, M.; Garzon, F.; Wood, D.; Zelenay, P.; More, K.; Stroh, K.; Zawodzinski, T.; Boncella, J.; McGrath, J. E.; Inaba, M.; Miyatake, K.; Hori, M.; Ota, K.; Ogumi, Z.; Miyata, S.; Nishikata, A.; Siroma, Z.; Uchimoto, Y.; Yasuda, K.; Kimijima, K.-i.; Iwashita, N. Scientific Aspects of Polymer Electrolyte Fuel Cell Durability and Degradation. *Chem. Rev.* **2007**, *107*, 3904−3951.
(16) Li, D.; Matanovic, I.; Lee, A. S.; Park, E. J.; Fujimoto, C.; Chung, H. T.; Kim, Y. S. Phenyl Oxidation Impacts the Durability of Alkaline Membrane Water Electrolyzer. *ACS Appl. Mater. Interfaces* **2019**, *11*, 9696−9701.
(17) Park, E. J.; Maurya, S.; Hibbs, M. R.; Fujimoto, C. H.; Kreuer, K.-D.; Kim, Y. S. Alkaline Stability of Quaternized Diels−Alder Polyphenylenes. *Macromolecules* **2019**, *52*, 5419−5428.
(18) Fan, J.; Willdorf-Cohen, S.; Schibli, E. M.; Paula, Z.; Li, W.; Skalski, T. J. G.; Sergeenko, A. T.; Hohenadel, A.; Frisken, B. J.; Magliocca, E.; Mustain, W. E.; Diesendruck, C. E.; Dekel, D. R.; Holdcroft, S. Poly(bis-arylimidazoliums) Possessing High Hydroxide Ion Exchange Capacity and High Alkaline Stability. *Nat. Commun.* **2019**, *10*, No. 2306.
(19) Tao, H. B.; Xu, Y.; Huang, X.; Chen, J.; Pei, L.; Zhang, J.; Chen, J. G.; Liu, B. A General Method to Probe Oxygen Evolution Intermediates at Operating Conditions. *Joule* **2019**, *3*, 1498−1509.
(20) Cao, X.; Novitski, D.; Holdcroft, S. Visualization of Hydroxide Ion Formation upon Electrolytic Water Splitting in an Anion Exchange Membrane. *ACS Mater. Lett.* **2019**, *1*, 362−366.
(21) Wright, A. G.; Fan, J.; Britton, B.; Weissbach, T.; Lee, H.-F.; Kitching, E. A.; Peckham, T. J.; Holdcroft, S. Hexamethyl-p-terphenyl Poly(benzimidazolium): A Universal Hydroxide-Conducting Polymer for Energy Conversion Devices. *Energy Environ. Sci.* **2016**, *9*, 2130−2142.
(22) Kaczur, J. J.; Yang, H.; Liu, Z.; Sajjad, S. D.; Masel, R. I. Carbon Dioxide and Water Electrolysis Using New Alkaline Stable Anion Membranes. *Front. Chem.* **2018**, *6*, No. 263.
(23) Wang, J.; Zhao, Y.; Setzler, B. P.; Rojas-Carbonell, S.; Ben Yehuda, C.; Amel, A.; Page, M.; Wang, L.; Hu, K.; Shi, L.; Gottesfeld, S.; Xu, B.; Yan, Y. Poly(aryl piperidinium) Membranes and Ionomers for Hydroxide Exchange Membrane Fuel Cells. *Nat. Energy* **2019**, *4*, 392−398.
(24) Sauerbrey, G. Z. Use of Quartz Vibration for Weighing Thin Films on a Microbalance. *Physica A* **1959**, *155*, 206−222.
(25) Winget, P.; Weber, E. J.; Cramer, C. J.; Truhlar, D. G. Computational Electrochemistry: Aqueous One-Electron Oxidation Potentials for Substituted Anilines. *Phys. Chem. Chem. Phys.* **2000**, *2*, 1231−1239.

(26) Epsztein, R.; Shaulsky, E.; Qin, M.; Elimelech, M. Activation Behavior for Ion Permeation in Ion-Exchange Membranes: Role of Ion Dehydration in Selective Transport. *J. Membr. Sci.* **2019**, *580*, 316−326.
(27) Koch, S.; Heizmann, P. A.; Kilian, S. K.; Britton, B.; Holdcroft, S.; Breitwieser, M.; Vierrath, S. The Effect of Ionomer Content in Catalyst Layers in Anion-Exchange Membrane Water Electrolyzers Prepared with Reinforced Membranes (Aemion$^+$). *J. Mater. Chem. A* **2021**, *9*, 15744−15754.
(28) Duffin, A. M.; Schwartz, C. P.; England, A. H.; Uejio, J. S.; Prendergast, D.; Saykally, R. J. pH-Dependent X-ray Absorption Spectra of Aqueous Boron Oxides. *J. Chem. Phys.* **2011**, *134*, No. 154503.
(29) Zhou, Y.; Yamaguchi, T.; Zhang, W.; Ikeda, K.; Yoshida, K.; Zhu, F.; Liu, H. The Structural Elucidation of Aqueous H_3BO_3 Solutions by DFT and Neutron Scattering Studies. *Phys. Chem. Chem. Phys.* **2020**, *22*, 17160−17170.
(30) Luo, X.; Kushner, D. I.; Li, J.; Park, E. J.; Kim, Y. S.; Kusoglu, A. Anion Exchange Ionomers: Impact of Chemistry on Thin-Film Properties. *Adv. Funct. Mater.* **2021**, *31*, No. 2008778.
(31) Moulder, J. F.; Stickle, W. F.; E'Sobol, P.; Bomben, K. D. *Handbook of X-Ray Photoelectron Spectroscopy*; Perkin-Elmer Corporation, 1992; pp 252−253.
(32) Thomas, O. D.; Soo, K. J. W. Y.; Peckham, T. J.; Kulkarni, M. P.; Holdcroft, S. A Stable Hydroxide-Conducting Polymer. *J. Am. Chem. Soc.* **2012**, *134*, 10753−10756.
(33) Lindquist, G. A.; Xu, Q.; Oener, S. Z.; Boettcher, S. W. Membrane Electrolyzers for Impure-Water Splitting. *Joule* **2020**, *4*, 2549−2561.
(34) Hübner, G.; Roduner, E. EPR Investigation of HO Radical Initiated Degradation Reactions of Sulfonated Aromatics as Model Compounds for Fuel Cell Proton Conducting Membranes. *J. Mater. Chem.* **1999**, *9*, 409−418.
(35) Kiessling, A.; Fornaciari, J. C.; Anderson, G.; Peng, X.; Gerstmayr, A.; Gerhardt, M. R.; McKinney, S.; Serov, A.; Kim, Y. S.; Zulevi, B.; Weber, A. Z.; Danilovic, N. Influence of Supporting Electrolyte on Hydroxide Exchange Membrane Water Electrolysis Performance: Anolyte. *J. Electrochem. Soc.* **2021**, *168*, No. 084512.
(36) Pellerite, M.; Kaplun, M.; Hartmann-Thompson, C.; Lewinski, K. A.; Kunz, N.; Gregar, T.; Baetzold, J.; Lutz, D.; Quast, M.; Liu, Z.; Yang, H.; Sajjad, S. D.; Gao, Y.; Masel, R. Imidazolium-Functionalized Polymer Membranes for Fuel Cells and Electrolyzers. *ECS Trans.* **2017**, *80*, 945−956.
(37) Liu, Z.; Yang, H.; Kutz, R.; Masel, R. I. CO_2 Electrolysis to CO and O_2 at High Selectivity, Stability and Efficiency Using Sustainion Membranes. *J. Electrochem. Soc.* **2018**, *165*, J3371−J3377.
(38) Luo, X.; Rojas-Carbonell, S.; Yan, Y.; Kusoglu, A. Structure-Transport Relationships of Poly(aryl piperidinium) Anion-Exchange Membranes: Effect of Anions and Hydration. *J. Membr. Sci.* **2020**, *598*, No. 117680.
(39) Endrődi, B.; Kecsenovity, E.; Samu, A.; Halmágyi, T.; Rojas-Carbonell, S.; Wang, L.; Yan, Y.; Janáky, C. High Carbonate Ion Conductance of a Robust PiperION Membrane Allows Industrial Current Density and Conversion in a Zero-Gap Carbon Dioxide Electrolyzer Cell. *Energy Environ. Sci.* **2020**, *13*, 4098−4105.
(40) Gabla, J. J.; Mistry, S. R.; Maheria, K. C. An Efficient Green Protocol for the Synthesis of Tetra-Substituted Imidazoles Catalyzed by Zeolite BEA: Effect of Surface Acidity and Polarity of Zeolite. *Catal. Sci. Technol.* **2017**, *7*, 5154−5167.
(41) Thavamani, S.; Amaladhas, T. Encapsulation of Cu(II), Ni(II) and V(IV) -Imidazole Complexes in Fly Ash Zeolite, Characterisation and Catalytic Activity towards Hydroxylation of Phenol. *J. Mater. Environ. Sci.* **2016**, *7*, 2314−2327.

https://doi.org/10.1021/acsami.1c22472
ACS Appl. Mater. Interfaces 2022, 14, 18261−18274